JACS
JOURNAL OF THE AMERICAN CHEMICAL SOCIETY

Article

pubs.acs.org/JACS

# Relative Order of Sulfuric Acid, Bisulfate, Hydronium, and Cations at the Air−Water Interface

Wei Hua, Dominique Verreault, and Heather C. Allen*

Department of Chemistry & Biochemistry, The Ohio State University, 100 West 18th Avenue, Columbus, Ohio 43210, United States

Supporting Information

**ABSTRACT:** Sulfuric acid ($H_2SO_4$), bisulfate ($HSO_4^-$), and sulfate ($SO_4^{2-}$) are among the most abundant species in tropospheric and stratospheric aerosols due to high levels of atmospheric $SO_2$ emitted from biomass burning and volcanic eruptions. The air/aqueous interfaces of sulfuric acid and bisulfate solutions play key roles in heterogeneous reactions, acid rain, radiative balance, and polar stratospheric cloud nucleation. Molecular-level knowledge about the interfacial distribution of these inorganic species and their perturbation of water organization facilitates a better understanding of the reactivity and growth of atmospheric aerosols and of the aerosol surface charge, thus shedding light on topics of air pollution, climate change, and thundercloud electrification. Here, the air/aqueous interface of $NaHSO_4$, $NH_4HSO_4$, and $Mg(HSO_4)_2$ salt solutions as well as $H_2SO_4$ and HCl acid solutions are investigated by means of vibrational sum frequency generation (VSFG) and heterodyne-detected (HD) VSFG spectroscopy. VSFG spectra of all acid solutions show higher SFG response in the OH-bonded region relative to neat water, with 1.1 M $H_2SO_4$ being more enhanced than 1.1 M HCl. In addition, VSFG spectra of bisulfate salt solutions highly resemble that of the dilute $H_2SO_4$ solution (0.26 M) at a comparable pH. HD-VSFG (Im $\chi^{(2)}$) spectra of acid and bisulfate salt solutions further reveal that hydrogen-bonded water molecules are oriented preferentially toward the bulk liquid phase. General agreement between Im $\chi^{(2)}$ spectra of 1.1 M $H_2SO_4$ and 1.1 M HCl acid solutions indicate that $HSO_4^-$ ions have a similar surface preference as that of chloride ($Cl^-$) ions. By comparing the direction and magnitude of the electric fields arising from the interfacial ion distributions and the concentration of each species, the most reasonable relative surface preference that can be deduced from a simplified model follows the order $H_3O^+ > HSO_4^- > Na^+, NH_4^+, Mg^{2+} > SO_4^{2-}$. Interestingly, contrary to some other near-neutral salt solution interfaces (e.g., chlorides and nitrates), cation-specific effects are here overshadowed by hydronium ions.

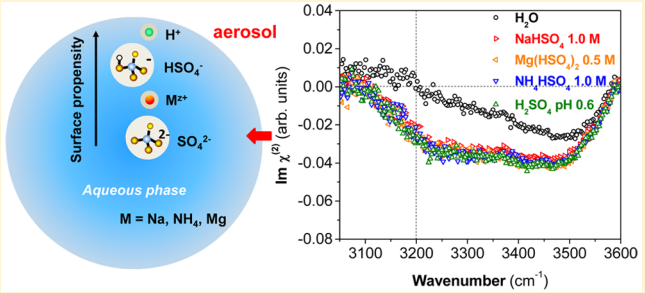


## INTRODUCTION

Sulfur species, existing in the form of sulfuric acid ($H_2SO_4$), bisulfate ($HSO_4^-$), and sulfate ($SO_4^{2-}$) depending on the solution pH, are among the most abundant inorganic components in lower (troposphere) and upper (stratosphere) atmospheric aerosols.[1,2] The concentration of $H_2SO_4$ in lower atmospheric aerosols is typically greater than 40 wt % and can be neutralized by ammonia.[3] Sulfate-containing aerosols emitted from man-made and naturally occurring sources play key roles in atmospheric heterogeneous reactions, acid rain, secondary organic aerosol chemistry, radiative forcing, and polar stratospheric cloud nucleation,[1,2,4−8] which in turn impact levels of atmospheric pollution, climate change, and stratospheric ozone depletion, respectively. For instance, the heterogeneous hydrolysis of $N_2O_5$ on the surface of $H_2SO_4$, $NH_4HSO_4$, and $(NH_4)_2SO_4$-containing aerosols[9−11] leads to the formation of nitric acid which influences the $NO_x$ cycle and, in turn, is associated with stratospheric ozone depletion.[12] $H_2SO_4$ and $HSO_4^-$ are also found to play a role in aerosol homogeneous nucleation, thus impacting lower and upper atmospheric chemistry.[13−15] The air/aqueous interface of atmospheric aerosols provide reaction sites that control the uptake, growth, and reactivity of the aerosol. Surface charge of atmospheric aerosols may also play a key role in thundercloud electrification.[16] In order to better understand these phenomena, it is imperative to gain molecular insight into the interfacial ion distribution of the relevant inorganic sulfur species, as is presented in this work.

Although numerous experimental and theoretical studies have been carried out to elucidate the interfacial distribution of $H_2SO_4$ and $SO_4^{2-}$ ions and their impact on water's hydrogen-bonding network at the bare air/aqueous interface, there are still more questions than answers. Using Auger electron and X-ray photoelectron spectroscopies, Somorjai and co-workers found that sulfuric acid (≤15 wt %) surface chemical composition reflects that of the bulk at room temperature.[17] Shortly after, the groups of Shen and Shultz independently measured the first vibrational spectra of the interface of sulfuric acid solutions using vibrational sum frequency generation (VSFG) spectroscopy.[18,19] A similar concentration dependence of the SFG response in the water OH stretching region (3000−

Received: August 14, 2015
Published: October 10, 2015





DOI: 10.1021/jacs.5b08636
J. Am. Chem. Soc. 2015, 137, 13920−13926

3800 $cm^{-1}$) was reported. The broad region (3000−3600 $cm^{-1}$) associated with hydrogen-bonded water molecules showed an intensity increase up to 0.02$x$ (mole fraction, ∼1.1 M) followed by a decrease at higher concentrations, while the 3700 $cm^{-1}$ peak related to the dangling OH of surface water molecules invariably decreased with addition of sulfuric acid. For spectra at low concentrations (<0.1$x$), Shen and co-workers interpreted the signal enhancement as due to the presence of crystal-like ordered $H_2SO_4{\cdot}H_2O$ structures at the aqueous surface,[18] whereas Shultz and co-workers explained the results as due to the water orientation caused by the formation of an electric double layer (EDL).[19]

Recently, Morita and co-workers combined VSFG spectroscopy and molecular dynamic (MD) simulations to provide insight into the interfacial ion distribution of sulfuric acid solution.[20−22] They postulated that in dilute solutions (<0.02$x$) ion surface composition is nearly identical to that found in the bulk and that ion surface preference follows the order hydronium ($H_3O^+$) > $HSO_4^-$ > $SO_4^{2-}$.[21] The surface enrichment of $H_3O^+$ ions[23−27] as well the strong repulsion of $SO_4^{2-}$ from the air/water interface[28−35] has been documented with various computational and experimental work; however, there is a dearth of information regarding the surface propensity of $HSO_4^-$.[21]

Unlike $H_2SO_4$ and $SO_4^{2-}$ ion, very few studies have investigated the solvation structure and ion partitioning of $HSO_4^-$, a weak acid ($pK_a$ ∼ 2.0)[36] in aqueous solution. Work on gas-phase bisulfate anion clusters suggested the enhanced incorporation of $HSO_4^-$'s hydrogen atom into the hydrogen-bonding network by binding to an acceptor-like water molecule.[37] In the water OH stretching region, Shultz and co-workers observed a greater SFG response in the VSFG spectra of 0.01$x$ alkali metal ($Li^+$, $K^+$, $Cs^+$) bisulfate salt solutions, particularly on the low frequency side (3000−3300 $cm^{-1}$), an increase that they attributed to the formation of a subsurface EDL and to the closer penetration of anions to the surface relative to cations.[28,38] Jubb and Allen further proposed that countercations such as $Na^+$ and $Mg^{2+}$ disturb $HSO_4^-$ hydration differently compared to $H_3O^+$, resulting in a blue-shift of the $SO_3$ symmetric stretching mode frequency, with $Mg^{2+}$ exerting a greater perturbation than $Na^+$.[39] However, the impact of $H_3O^+$ as well as that of countercations on the surface preference of $HSO_4^-$ has yet to be explored.

Here, we employ both VSFG spectroscopy and its phase-resolved variant, heterodyne-detected (HD-) VSFG, to gain molecular-level information regarding $HSO_4^-$ ion interfacial distribution and that of its countercations ($Na^+$, $NH_4^+$, $Mg^{2+}$). In addition, we examined the influence of $H_2SO_4$ and bisulfate salts on the interfacial water hydrogen-bonding network, in particular the net dipole orientation of water molecules, which still remain largely unknown. Our findings reveal that $HSO_4^-$ ions on average have a similar ion distribution as that of $Cl^-$ ions. We propose that the relative surface preference at air/acidic bisulfate salt solution interfaces follow the order $H_3O^+$ > $HSO_4^-$ > $Na^+$, $NH_4^+$, $Mg^{2+}$ > $SO_4^{2-}$, while the impact of countercations is surpassed by $H_3O^+$ ions.

## EXPERIMENTAL DETAILS

**Materials.** Sodium bisulfate monohydrate ($NaHSO_4$; crystalline/certified, Fisher Scientific), ammonium sulfate ($(NH_4)_2SO_4$; ACS reagent, ≥99%, Acros Organics), magnesium sulfate anhydrous ($MgSO_4$; powder/certified, Fisher Scientific), sulfuric acid ($H_2SO_4$; trace metal grade, Fisher Scientific), and hydrochloric acid (HCl; trace metal grade, Fisher Scientific) were purchased from different suppliers. Ultrapure water (not purged of $CO_2$) with a resistivity of 18.2−18.3 MΩ·cm and a measured pH of 5.6 was obtained from a Barnstead Nanopure system (model D4741, Thermolyne Corporation) equipped with additional organic removing cartridges (D5026 Type I ORGANICfree Cartridge Kit; Pretreat Feed).

**Preparation of Salt Solutions.** Stock salt and acid solutions for VSFG measurements were prepared by dissolving ACS grade salts and trace metal grade acids in ultrapure water. Owing to its ultrahigh sensitivity, VSFG spectra obtained in the surfactant CH stretching region (2800−3000 $cm^{-1}$) were utilized as a probe to verify the presence of trace amount organic contaminants. As revealed in these spectra, organic contamination was found in stock salt solutions prior to any pretreatment.[40] To completely eliminate organic impurities, $NaHSO_4$, $(NH_4)_2SO_4$, and $MgSO_4$ stock solution was filtered three times using activated carbon filters (Whatman Carbon Cap 75, Fisher Scientific). After thorough removal of organic contamination, for the same inorganic salt, solutions made from ACS and ultrapure grade salts (trace metal basis, purities ranging from 99.99 to 99.9999%) perturb the VSFG and HD-VSFG spectra in the water OH stretching region mostly to the same extent.[40] The pretreated (filtered) $NaHSO_4$, $(NH_4)_2SO_4$, and $MgSO_4$ stock salt solutions were shown to be free of organic impurities as revealed by VSFG spectra obtained in the CH stretching region (Supporting Information).[40,41] Raman calibration curves were obtained to determine the concentration of bisulfate and sulfate salt solutions after filtration based on vibrational symmetric stretch modes of $HSO_4^-$ (∼1052 $cm^{-1}$) and $SO_4^{2-}$ (∼982 $cm^{-1}$) ions (see Supporting Information). After pretreatment and Raman calibration, the $NaHSO_4$ stock solution was directly diluted to the desired concentration (1.0 M), while 1.0 M $NH_4HSO_4$ and 1.0 M $Mg(HSO_4)_2$ were prepared by stoichiometrically mixing (1:1 molar ratio) stock solutions of $(NH_4)_2SO_4$ and $MgSO_4$ with $H_2SO_4$. The measured pH of 1.0 M $NaHSO_4$, 1.0 M $NH_4HSO_4$, and 1.0 M $Mg(HSO_4)_2$ was 0.7 ± 0.1 (±0.05 M [$H_3O^+$]). The Debye lengths were calculated to be ∼0.3 nm, and thus solutions can be compared. The Debye length for the pH 0.6 $H_2SO_4$ solution is ∼0.6 nm. All solutions were thermally equilibrated to room temperature (23 ± 1 °C) over 24 h before use. No degassing or $N_2$ purging has been applied on them.

**VSFG Spectroscopy.** VSFG spectroscopy measurements were performed on a broad-bandwidth VSFG spectrometer setup which has been described in detail elsewhere.[42,43] In contrast to VSFG spectroscopy that measures the squared absolute value of the second-order nonlinear susceptibility ($\chi^{(2)}$), HD-VSFG spectroscopy provides both the real (Re) and imaginary (Im) parts of $\chi^{(2)}$ based on the interference of the sample SFG response with that of a phase reference. The sign of Im $\chi^{(2)}$ relates directly to the net dipole orientation of interfacial water molecules.[44,45] The HD-VSFG spectroscopy setup is mostly based on "conventional" VSFG, with the optical configuration in the sample stage area redesigned for the new application.[33,46] The latter setup is similar to the system reported by Tahara and co-workers,[45] which is based on heterodyne detection of broad bandwidth signals and Fourier transform analysis. The HD-VSFG setup and the data processing procedure have been described elsewhere in detail.[33,46−49] Here, only the modifications made to the experimental setup and calculated parameters are presented. Briefly, the full spectral bandwidth of the generated broadband infrared beam has been expanded from 3000 to 3600 $cm^{-1}$ (∼600 $cm^{-1}$) in the current HD-VSFG setup in the OH stretching region. The average incident energy of the visible (800 nm) and infrared (OH stretching region) beams prior to the sample stage was reduced to 260 and 8 μJ, respectively. The primary SF beam is time-delayed by 1.7 ps by its passage through a thin silica plate (<1 mm). Neat water spectra were used as a reference for salt comparison to assess reproducibility during the whole experimental period. Critical here is that all Im $\chi^{(2)}$ spectra of salt solutions are compared to that of neat water. Thus, our interpretation is based on the *relative* difference between neat water and the salt solutions. To check the validity in the general trend of these spectra, the deduced $|\chi^{(2)}|^2$ power spectra of each salt and acid solution reconstructed from the HD-VSFG results were compared to


DOI: 10.1021/jacs.5b08636
J. Am. Chem. Soc. 2015, 137, 13920−13926

those measured directly by conventional VSFG spectroscopy (see Supporting Information). Only every fourth data points are plotted in the HD-VSFG spectra to avoid spectral clutter. All the VSFG and HD-VSFG spectra are measured under the *ssp* (for sum frequency (*s*), visible (*s*), and infrared (*p*) beams, respectively) polarization combination.

## RESULTS AND DISCUSSION

**Impact of $H_2SO_4$ and Bisulfate Salts on the Interfacial Water Hydrogen-Bonding Network.** Figure 1A shows the

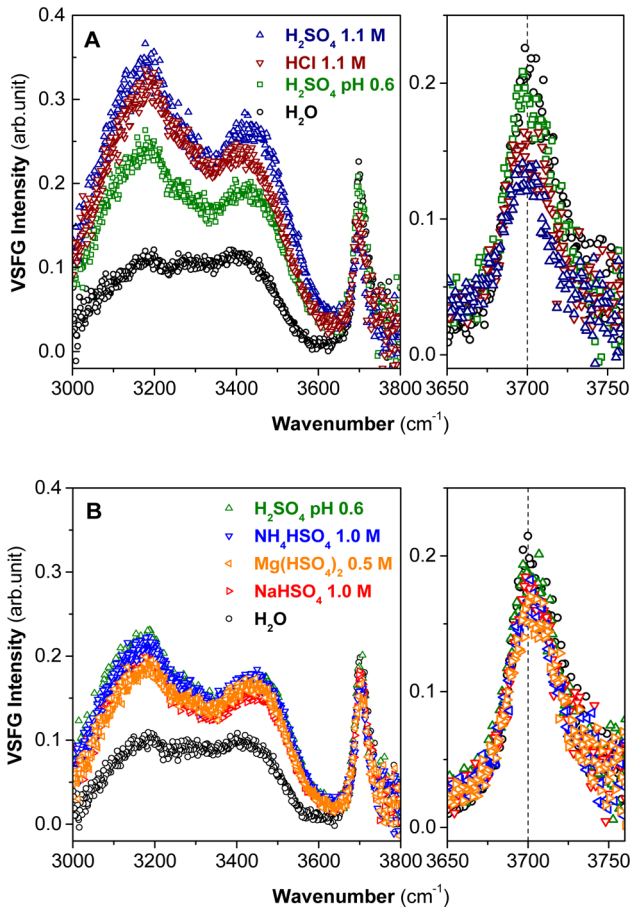


**Figure 1.** VSFG $|\chi_{eff}^{(2)}|^2$ spectra of the air/aqueous interfaces of (A) 1.1 M $H_2SO_4$, 1.1 M HCl, pH 0.6 (0.26 M) $H_2SO_4$ acid solutions, and (B) pH 0.6 $H_2SO_4$ acid solution, 1.0 M $NH_4HSO_4$, 0.5 M $Mg(HSO_4)_2$, and 1.0 M $NaHSO_4$ salt solutions over the entire OH stretching region (3000−3800 $cm^{-1}$). A neat water spectrum is shown as a reference. Data shown were measured on different days and hence demonstrate slight signal intensity difference due to normalization. High reproducibility during the entire experimental period within each day ensure a reliable comparison among samples.

VSFG spectra of the interfacial region of neat water, $H_2SO_4$, and HCl acid solutions measured in the OH stretching region (3000−3800 $cm^{-1}$). The interfacial region refers hereafter to the region which lacks inversion symmetry, hence SFG-active. In the case of neat water, only the topmost layers (∼1−3) are believed to be responsible for the observed SFG signal, while the adjacent sublayers make little contribution;[44,50] however, the presence of ions extends the region of noncentrosymmetry by forming an ionic double layer and hence generating an interfacial electric field. The direction and relative strength of this ion-induced electric field govern the interfacial water organization that involves both reorientation and restructuring of the water hydrogen-bond network which, in turn, leads to an increase in the interfacial depth, i.e., to a greater number of water molecules probed due to their SFG activity. The neat water $|\chi_{eff}^{(2)}|^2$ spectrum consists of a broad region spanning from 3000 to 3600 $cm^{-1}$ representing water molecules with a broad continuum of hydrogen bond lengths and a narrow band at 3700 $cm^{-1}$ assigned to the distinct dangling OH bond of water molecules located directly at the surface.[51] It is accepted that hydrogen bonds are relatively strong in the lower frequency part of the broad region, and as one moves to higher frequency, the hydrogen bond strength weakens significantly.[52,53] Additional assignments to this broad continuum continue to be debated.[54−57]

The VSFG spectra of 0.26 and 1.1 M $H_2SO_4$ and 1.1 M HCl acid solutions show an uneven increase in SFG signal intensity relative to that of neat water across the entire broad OH stretching region with increasing acid concentration (Figure 1A). The VSFG spectrum of the 1.1 M HCl acid solution resembles that of the 1.1 M $H_2SO_4$, albeit with a slightly lower intensity. A significant intensity decrease of the dangling OH peak with respective to neat water can be observed in the presence of 1.1 M acid solutions with $H_2SO_4$ having more effect than HCl (Figure 1A, right panel). The results of acid solutions are consistent with those previously published in the same concentration range.[18,19,25−27,38] The intensity enhancement of the broad OH stretching region suggests that the overall population of hydrogen-bonded water species that contribute to the SFG signal may increase. Considering that both HCl ($pK_a = -7.3$) and $H_2SO_4$ are strong acids ($pK_{a1} \sim -6$, $pK_{a2} \sim 2.0$),[36] the concentrations of $H_3O^+$ ions generated from the dissociation of 1.1 M HCl and from the first dissociation of 1.1 M $H_2SO_4$ are comparable. Thus, the small difference observed between the VSFG spectra of these two acid solutions may indicate a similar interfacial ion behavior of $HSO_4^-$ and $Cl^-$ because the concentrations of $H_3O^+$ and $SO_4^{2-}$ ions generated from the second dissociation amount to only ∼0.01 M, 2 orders of magnitude smaller than $HSO_4^-$.

To further investigate the interfacial behavior of $HSO_4^-$ ions, VSFG spectra of a series of $HSO_4^-$ salt solutions including 1.0 M $NaHSO_4$, 1.0 M $NH_4HSO_4$, and 0.5 M $Mg(HSO_4)_2$ as well as from a dilute 0.26 M $H_2SO_4$ acid solution are obtained. As seen in Figure 1B, all these $HSO_4^-$ salt solutions perturb the broad OH stretching region similar to that of the 0.26 M $H_2SO_4$ acid solution. This is generally in accordance with the previous VSFG results from other $HSO_4^-$ salt solutions in this concentration range,[28,31,38] although this is the first report about $NH_4HSO_4$ and $Mg(HSO_4)_2$ in the OH stretching region. The intensity of the dangling OH peak of these $HSO_4^-$ salt and dilute $H_2SO_4$ solutions appears to decrease slightly compared to that of neat water. The small difference in the broad OH stretching region may be attributed to the small pH variation of these solutions. The measured pH values of these salt and dilute acid solutions are highly comparable (pH 0.7 ± 0.1). Depending on their intrinsic properties, cations exert specific effects on the interfacial water organization in near-neutral chloride and nitrate salt solutions.[32,48,49,58] Interestingly, this cation-specific effect is much less pronounced here in acidic $HSO_4^-$ salt solutions. The increased complexity of the system due to the presence of $H_3O^+$ ions makes it more difficult to explore the interfacial $HSO_4^-$ ion behavior and distribution in the bisulfate salt solutions.


DOI: 10.1021/jacs.5b08636
J. Am. Chem. Soc. 2015, 137, 13920−13926

**$H_2SO_4$ and Bisulfate Salt Effects on the Interfacial Electric Field.** In contrast to VSFG, HD-VSFG allows for a direct interrogation of the sign of Im $\chi^{(2)}$, which reflects the net orientation of the water OH transition dipole moment of SFG-active OH vibrational stretching modes. Additionally, HD-VSFG spectroscopy not only provides resonance information but also excludes the contribution of possible interference effects from the nonresonant background and convolution effects between the real and imaginary parts of $\chi^{(2)}$. Therefore, it is advantageous to employ HD-VSFG spectroscopy to investigate the complex $HSO_4^-$ salt solutions.

The Im $\chi^{(2)}$ spectrum of the neat air/water in the OH stretching region is shown in Figure 2 and is consistent with those previously reported.[27,44,45] The sign of the Im $\chi^{(2)}$ spectrum of neat water in the 3000−3200 $cm^{-1}$ region is positive, suggesting that the OH stretch net transition dipole moment is oriented toward the surface; however, the assignments for this region remain controversial.[54−57,59] In contrast, the Im $\chi^{(2)}$ spectrum from 3200 to 3600 $cm^{-1}$ reveals a negative band, and this spectral region has been explicitly attributed to OH stretches with a net transition dipole moment oriented on average toward the isotropic bulk solution although the orientational distribution is likely to be broad. We focus predominately on this region for spectral interpretation.

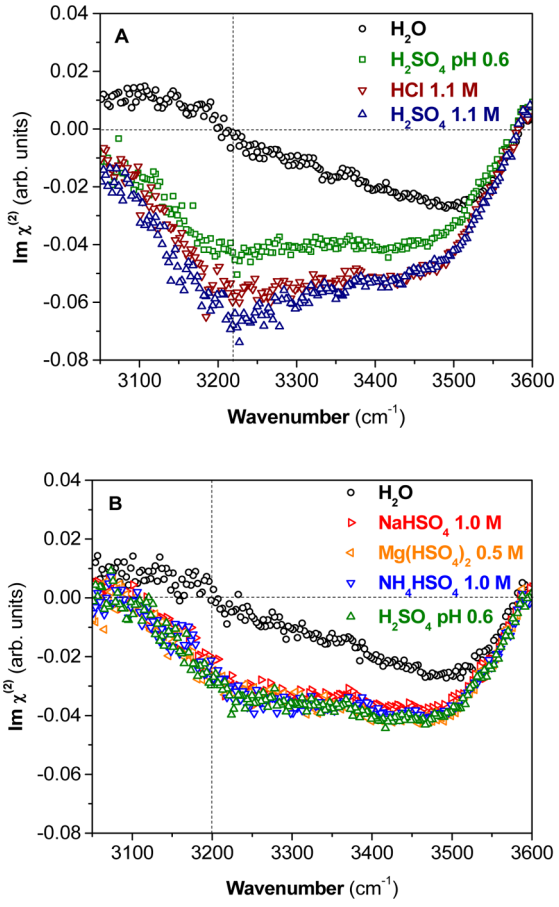


**Figure 2.** HD-VSFG Im $\chi^{(2)}$ spectra of air/aqueous interfaces of (A) 1.1 M $H_2SO_4$, 1.1 M HCl, pH 0.6 (0.26 M) $H_2SO_4$ acid solutions and (B) pH 0.6 $H_2SO_4$ acid solution and 1.0 M $NH_4HSO_4$, 0.5 M $Mg(HSO_4)_2$, and 1.0 M $NaHSO_4$ salt solutions over the OH stretching region (3000−3600 $cm^{-1}$). A neat water spectrum is shown as a reference. Data shown were measured on different days and hence demonstrates slight signal intensity difference due to normalization.

Similar to the perturbation observed in the VSFG spectra (Figure 1A), the partitioning of $H_3O^+$ ions and its counter-anions $HSO_4^-$ and $Cl^-$ in the interfacial region leads to significant spectral changes in the corresponding Im $\chi^{(2)}$ spectra (Figure 2A). Relative to neat water, the sign of the Im $\chi^{(2)}$ spectra in the lower frequency region (3000−3200 $cm^{-1}$) changes from positive to negative and an enhancement of the signal intensity is observed in the higher frequency region (3200−3550 $cm^{-1}$) for all acid solutions. To date, there has been no published Im $\chi^{(2)}$ spectrum from the bare air/$H_2SO_4$ acid solution interface. The Im $\chi^{(2)}$ spectrum of the air/aqueous interface of 1.1 M HCl acid solution agrees with the one previously reported by Shen and co-workers.[27] The overall negative signal enhancement observed for all acid solutions from 3200 to 3500 $cm^{-1}$ is likely associated with the reorganization of the interfacial water molecules with their net transition dipole moment oriented more toward the bulk solution. This reorganization can be physically explained by the generation of a negative interfacial electric field between the $H_3O^+$ ions residing on average predominately above their $Cl^-$ and/or $HSO_4^-$ counteranions, closer to the surface. This molecular picture reveals the formation of a double-layer structure.[25−27,38] Analogous to the VSFG spectrum, the perturbation of the Im $\chi^{(2)}$ spectrum by $H_2SO_4$ shows a concentration dependency, having more enhancement in the negative signal intensity with increasing acid concentration.

One can note that analogous to the VSFG spectra in Figure 1A, the Im $\chi^{(2)}$ spectra of the 1.1 M HCl and $H_2SO_4$ acid solutions in Figure 2A also display high resemblance while that of $H_2SO_4$ has a slightly more negative signal intensity in the lower frequency region between 3050 and 3300 $cm^{-1}$. As discussed above, the overall $H_3O^+$ ion concentrations in these two acid solutions only differs by ∼0.01 M (due to the additional dissociation of $HSO_4^-$). In addition to the dominating $HSO_4^-$ (1.1 M) and $H_3O^+$ (1.11 M) ions, a small amount of $SO_4^{2-}$ (∼0.01 M) ions also exists in the solution. $SO_4^{2-}$ ions have been suggested to preferentially reside deeper in the interfacial region[29−33] relative to $HSO_4^-$ ions.[21,39] The interfacial ion distribution of the $H_2SO_4$ acid solution is schematically illustrated in Figure 3A. It has been demonstrated that the Im $\chi^{(2)}$ spectra of $SO_4^{2-}$ salts have an enhanced negative signal intensity across most of the OH stretching region (3050−3500 $cm^{-1}$), indicating that $SO_4^{2-}$ reside below their countercations.[32,33] Moreover, the slight negative signal enhancement of $H_2SO_4$ relative to HCl can be attributed to two possible factors: (1) the presence of ∼0.01 M $H_3O^+$ and $SO_4^{2-}$ ions introduces another weak interfacial electric field; (2) different ion features of $HSO_4^-$ compared to $Cl^-$. For example, the hydrogen atom of $HSO_4^-$ may act as a hydrogen bond donor to a water molecule and thus disturb the hydrogen-bonding network.[37] Although it is difficult to estimate the exact contribution from each factor, the latter one may be dominant if one considers the low concentration of $SO_4^{2-}$ ions. Further theoretical study would aid in elucidating this question. Taking into account the nearly identical concentration of dominating ions and the similarity of the Im $\chi^{(2)}$ spectra of 1.1 M HCl and $H_2SO_4$ acid solutions, it is reasonable to assume that the ion distributions of $HSO_4^-$ and $Cl^-$ are comparable (Debye lengths are comparable as well). In other words, $HSO_4^-$ ions may have a similar surface preference as that of $Cl^-$ ions.


DOI: 10.1021/jacs.5b08636
J. Am. Chem. Soc. 2015, 137, 13920−13926

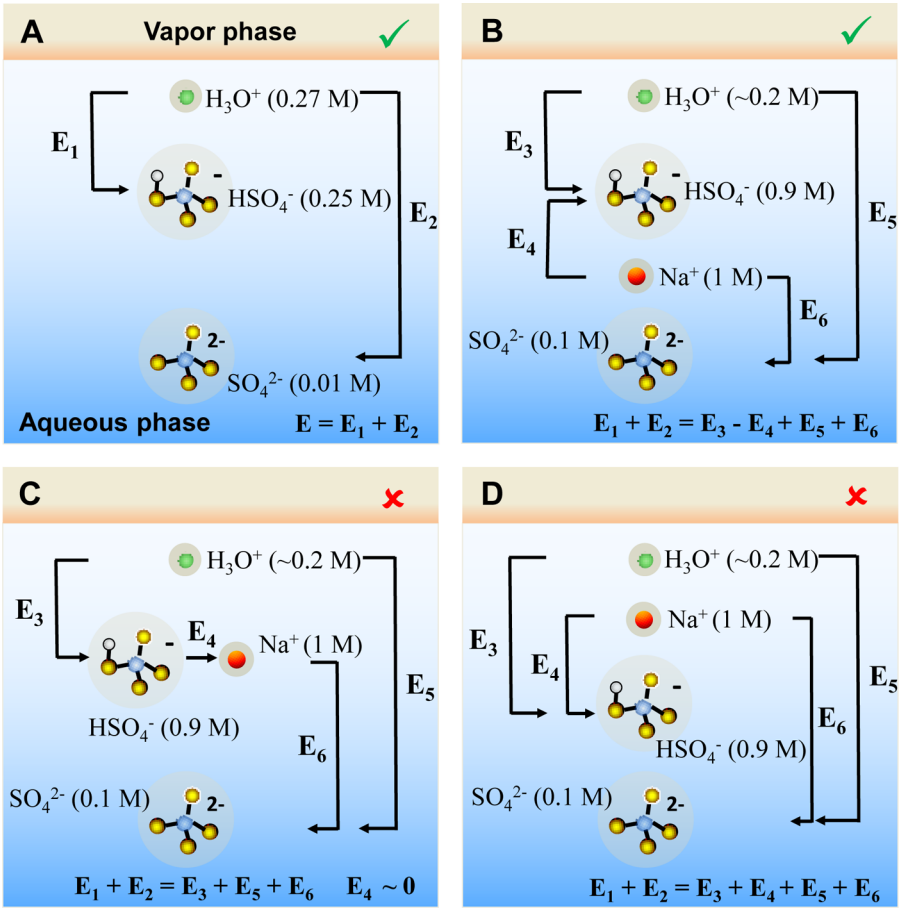


**Figure 3.** Possible scenarios of ion distributions at the interface of (A) pH 0.6 $H_2SO_4$ (0.26 M) acid solution and (B–D) of 1.0 M $NaHSO_4$ salt solution. The dilute $H_2SO_4$ solution and 1.0 M $NaHSO_4$ salt solution are of comparable pH value (same $[H_3O^+]$), and hence $E_1 \leq E_3$ and $E_2 \leq E_5$. If the ion distribution of the dilute $H_2SO_4$ solution is as the one shown in scenario A, then scenario B would be the only reasonable distribution after comparing the magnitude of all *E*-fields that exist in the system. (Note that scenarios B–D are not charge balanced due to the relative uncertainty in the pH measurement (±0.05 M in $[H_3O^+]$); however, the concentration of $HSO_4^-$ ions is more than 3 times larger (0.9 M vs 0.25 M) in scenarios B–D compared to scenario A; thus, $E_1 \leq E_3$ and $E_2 \leq E_5$ remain valid.)

To further elucidate the ion distribution of the complex $HSO_4^-$ salt solutions, the Im $\chi^{(2)}$ spectra of 1.0 M $NaHSO_4$, 1.0 M $NH_4HSO_4$, and 0.5 M $Mg(HSO_4)_2$ are measured (Figure 2B). A dilute 0.26 M $H_2SO_4$ acid solution with a comparable pH value as that of the $HSO_4^-$ salt solutions is used as a control. To the authors' knowledge, this is the first time that the Im $\chi^{(2)}$ spectra of $HSO_4^-$ salt solutions been reported. It is also important to note that although surface tension can be used to infer surface propensity,[62,63] it does not provide a definitive relative order or definitive position of ions at the air/aqueous interface as documented by many relatively recent studies.[64−66] Whereas the results examined here provide relative ordering, yet defining the absolute position of the ion distribution peak(s) still remains unresolved.

By looking closely at Figure 2B, one notices that the spectral line shape of the Im $\chi^{(2)}$ spectra of all 1.0 M $HSO_4^-$ salt solutions exhibit strong similarity to that of the 0.26 M $H_2SO_4$ acid solution, displaying a significant enhancement of the negative magnitude across the entire OH stretching region from 3050 to 3600 $cm^{-1}$. This implies that the net overall strength and direction of the interfacial electric fields in these acid and acidic salt solutions are mostly identical. To evaluate the direction and strength of each electric field generated by the presence of different groups of ions, it is critical to understand the ion distribution positions relative to each other. Since the ion distribution of the $H_2SO_4$ acid solution has been discussed, the question remaining now is the distribution of $HSO_4^-$ ions relative to the countercations.

**Ion Distribution Model.** To answer this question, a comparison of the surface electric fields that exist in the dilute 0.26 M $H_2SO_4$ and 1.0 M $NaHSO_4$ solutions is made as an example. In the case of the air/$HSO_4^-$ salt solution interface, there are three possible scenarios invoked: (1) $HSO_4^-$ ions residing on average above their countercations (Figure 3B), (2) $HSO_4^-$ and their countercations having similar distributions (Figure 3C), and (3) $HSO_4^-$ residing below the countercations (Figure 3D). The measured bulk pH value of the 1.0 M $NaHSO_4$ solution is ~0.7. After taking into account the dissociation of $HSO_4^-$ ion in each system, in the 0.26 M $H_2SO_4$ solution, the concentrations of $H_3O^+$, $HSO_4^-$, and $SO_4^{2-}$ are approximately 0.27, 0.25, and 0.01 M, respectively, while in the 1.0 M $NaHSO_4$ solution, the concentrations of $Na^+$, $HSO_4^-$, $H_3O^+$, and $SO_4^{2-}$ are approximately 1, 0.9, ~0.2 (based on measured pH with an uncertainty of ±0.05 M), and 0.1 M, respectively. As mentioned above, an electric field can be generated by the formation of an ionic double layer between positively and negatively charged ions. In the 0.26 M $H_2SO_4$ solution, the overall net electric field (*E*) consists of two subfields: $E_1$ (a negative field between $H_3O^+$ and $HSO_4^-$; the *E*-field direction is defined as going from the positive to the


DOI: 10.1021/jacs.5b08636
J. Am. Chem. Soc. 2015, 137, 13920−13926

negative charge distributions and its sign is positive when directed toward the vapor phase) and $E_2$ (a negative field between $H_3O^+$ and $SO_4^{2-}$) (Figure 3A). For the 1.0 M $NaHSO_4$ solution, the overall net electric field ($E$) is the summation of four different subfields, including $E_3$ (a negative field between $H_3O^+$ and $HSO_4^-$), $E_4$ (a field between $Na^+$ and $HSO_4^-$, the sign depends on the scenario adopted), $E_5$ (a negative field between $H_3O^+$ and $SO_4^{2-}$), and $E_6$ (a negative field between $Na^+$ and $SO_4^{2-}$).[32,33] Because the overall net electric field of these two solutions are comparable in magnitude, this means that $E = E_1 + E_2 = E_3 + E_4 + E_5 + E_6$. If one assumes a similar distribution of the same ions in different solutions while taking into account their respective concentrations, and neglecting opposing water orientations including solvation shell water molecules (SFG selection rules),[52,67,68] then the magnitude of these fields must obey the relations $E_1 \leq E_3$ and $E_2 \leq E_5$. All induced electric fields have the same direction except for the unknown $E_4$.

To balance the overall strength of the net electric field, the only reasonable scenario is to have $E_4$ with an opposite direction compared to the other subfields. This indicates that $HSO_4^-$ ions would reside preferentially above the counter-cation $Na^+$ ions as shown in Figure 3B. If $Na^+$ ions adopt a similar distribution as that of the $HSO_4^-$ ions or reside on average above them as shown in Figure 3C,D, $E_4$ would be of negligible magnitude or have the same direction as the other subfields. In such scenarios, the three above-mentioned relations cannot be satisfied. Therefore, by comparing the magnitude and direction of all the electric fields that exist in the acid and acidic salt solutions, it is clear that $HSO_4^-$ ions possess a stronger surface preference relative to $Na^+$ ions.

As discussed above, the fact that $HSO_4^-$ ions have a similar surface preference as $Cl^-$ ions leads one to think that $HSO_4^-$ likely has a stronger surface propensity with respect to their countercations.[32,33,49] Interestingly, the cation-specific effects which alter the perturbation of the interfacial hydrogen-bonding network observed in the Im $\chi^{(2)}$ spectra of near-neutral pH chloride and nitrate salt solutions[32,48,49,58] are negligible in the acidic $HSO_4^-$ salt solution. This suggests that $H_3O^+$ outcompetes the influence of cations.

## CONCLUSIONS

The relative surface preference of ions that exist in $HSO_4^-$ salt solutions is shown here to follow the order $H_3O^+ > HSO_4^- > Na^+, NH_4^+, Mg^{2+} > SO_4^{2-}$. This ordering was deduced from a model that compares the direction and magnitude of the electric fields arising from the different interfacial ion distributions and the concentration of each species. VSFG spectra of acid solutions revealed an increased signal in the entire broad OH stretching region relative to neat water, with 1.1 M $H_2SO_4$ being slightly more enhanced than 1.1 M HCl. The VSFG spectra of bisulfate salt solutions displayed a strong resemblance with that of the dilute $H_2SO_4$ solution (0.26 M) at a comparable pH, suggesting that these species disturb the interfacial water organization to the same extent. In addition, for the first time, it is shown that hydrogen-bonded water molecules in the $H_2SO_4$ and bisulfate salt solutions are oriented preferentially toward the bulk solution.

The high similarity between the Im $\chi^{(2)}$ spectra of 1.1 M $H_2SO_4$ and 1.1 M HCl acid solutions leads to the important conclusion that $HSO_4^-$ and $Cl^-$ ions have comparable interfacial distributions. The Im $\chi^{(2)}$ spectra of the dilute $H_2SO_4$ and 1.0 M $HSO_4^-$ salt solutions are nearly indistinguishable. Unlike other near-neutral pH salt solutions (e.g., chlorides and nitrates), negligible cation-specific effects observed here at the interface of acidic $HSO_4^-$ salt solutions suggest that the presence of $H_3O^+$ ions somehow dampens the influence of other cations present.

These results help to shed light on the chemistry of sulfate-containing aerosols where surface acidity, sulfate concentration, and interfacial distribution have been linked to important atmospheric processes such as the catalytic production of chlorine radicals and the formation of cloud condensation nuclei, among others.

## ASSOCIATED CONTENT

### Supporting Information

The Supporting Information is available free of charge on the ACS Publications website at DOI: 10.1021/jacs.5b08636.

VSFG spectra of neat water and filtered $NaHSO_4$ stock salt solutions in the CH stretching region; Raman calibration curves of $NaHSO_4$ solution; conventional VSFG spectra of GaAs and water and HD-VSFG Im $\chi^{(2)}$ spectra of water obtained through the entire experimental period demonstrating system and phase stability; the $|\chi^{(2)}|^2$ power spectra and Re $\chi^{(2)}$ spectra deduced from HD-VSFG of water molecules at air/aqueous acid and salt solution interfaces (PDF)

## AUTHOR INFORMATION


### Corresponding Author

*E-mail allen@chemistry.ohio-state.edu.


### Notes

The authors declare no competing financial interest.

## ACKNOWLEDGMENTS

The authors acknowledge the financial support of the National Science Foundation Center for Chemical Innovation "Center for Aerosol Impacts on Climate and the Environment" through Grants CHE-1305427, NSF CHE-1111762, and DOE-BES FG02-04ER15495. W.H. acknowledges Mr. Zishuai Huang for his assistance in setting up the HD-VSFG experiments, Ms. Ellen M. Adams for her assistance in the preparation of sample solutions, and Dr. Aaron M. Jubb for helpful discussions.

## REFERENCES


(1) Finlayson-Pitts, B. J.; Pitts Jr., J. N. *Chemistry of the Upper and Lower Atmosphere: Theory, Experiments and Applications*; Academic Press: San Diego, CA, 2000; p 969.

(2) Seinfeld, J. H.; Pandis, S. N. *Atmospheric Chemistry and Physics: From Air Pollution to Climate Change*; John Wiley and Sons, Inc.: Hoboken, NJ, 2006.

(3) Keene, W. C.; Sander, R.; Pszenny, A. A. P.; Vogt, R.; Crutzen, P. J.; Galloway, J. N. *J. Aerosol Sci.* **1998**, *29*, 339−356.

(4) Andreae, M. O.; Crutzen, P. J. *Science* **1997**, *276*, 1052−1058.

(5) Ravishankara, A. R. *Science* **1997**, *276*, 1058−1065.

(6) Claeys, M.; Wang, W.; Ion, A.; Kourtchev, I.; Gelencser, A.; Maenhaut, W. *Atmos. Environ.* **2004**, *38*, 4093−4098.

(7) Riccobono, F.; Schobesberger, S.; Scott, C. E.; Dommen, J.; Ortega, I. K.; Rondo, L.; Almeida, J.; Amorim, A.; Bianchi, F.; Breitenlechner, M.; David, A.; Downard, A.; Dunne, E. M.; Duplissy, J.; Ehrhart, S.; Flagan, R. C.; Franchin, A.; Hansel, A.; Junninen, H.; Kajos, M.; Keskinen, H.; Kupc, A.; Kurten, A.; Kvashin, A. N.; Laaksonen, A.; Lehtipalo, K.; Makhmutov, V.; Mathot, S.; Nieminen, T.; Onnela, A.; Petaja, T.; Praplan, A. P.; Santos, F. D.; Schallhart, S.; Seinfeld, J. H.; Sipila, M.; Spracklen, D. V.; Stozhkov, Y.; Stratmann, F.; Tome, A.; Tsagkogeorgas, G.; Vaattovaara, P.; Viisanen, Y.; Vrtala,




DOI: 10.1021/jacs.5b08636
J. Am. Chem. Soc. 2015, 137, 13920−13926

A.; Wagner, P. E.; Weingartner, E.; Wex, H.; Wimmer, D.; Carslaw, K. S.; Curtius, J.; Donahue, N. M.; Kirkby, J.; Kulmala, M.; Worsnop, D. R.; Baltensperger, U. *Science* **2014**, *344*, 717−721.
(8) Sipila, M.; Berndt, T.; Petaja, T.; Brus, D.; Vanhanen, J.; Stratmann, F.; Patokoski, J.; Mauldin, R. L., III; Hyvarinen, A.-P.; Lihavainen, H.; Kulmala, M. *Science* **2010**, *327*, 1243−1246.
(9) Hu, J. H.; Abbatt, J. P. D. *J. Phys. Chem. A* **1997**, *101*, 871−878.
(10) Robinson, G. N.; Worsnop, D. R.; Jayne, J. T.; Kolb, C. E.; Davidovits, P. *J. Geophys. Res.* **1997**, *102*, 3583−3601.
(11) Kane, S. M.; Caloz, F.; Leu, M. T. *J. Phys. Chem. A* **2001**, *105*, 6465−6470.
(12) Fahey, D. W.; Kawa, S. R.; Woodbridge, E. L.; Tin, P.; Wilson, J. C.; Jonsson, H. H.; Dye, J. E.; Baumgardner, D.; Borrmann, S.; Toohey, D. W.; Avallone, L. M.; Proffitt, M. H.; Margitan, J.; Loewenstein, M.; Podolske, J. R.; Salawitch, R. J.; Wofsy, S. C.; Ko, M. K. W.; Anderson, D. E.; Schoeber, M. R.; Chan, K. R. *Nature* **1993**, *363*, 509−514.
(13) Eisele, F. L.; Lovejoy, E. R.; Kosciuch, E.; Moore, K. F.; Mauldin, R. L.; Smith, J. N.; McMurry, P. H.; Iida, K. *J. Geophys. Res.* **2006**, *111*, D04305.
(14) Yu, F. Q.; Turco, R. P. *J. Geophys. Res.* **2001**, *106*, 4797−4814.
(15) Lee, S. H.; Reeves, J. M.; Wilson, J. C.; Hunton, D. E.; Viggiano, A. A.; Miller, T. M.; Ballenthin, J. O.; Lait, L. R. *Science* **2003**, *301*, 1886−1889.
(16) Jungwirth, P.; Rosenfeld, D.; Buch, V. *Atmos. Res.* **2005**, *76*, 190−205.
(17) Fairbrother, D. H.; Johnston, H.; Somorjai, G. *J. Phys. Chem.* **1996**, *100*, 13696−13700.
(18) Radüge, C.; Pflumio, V.; Shen, Y. R. *Chem. Phys. Lett.* **1997**, *274*, 140−144.
(19) Baldelli, S.; Schnitzer, C.; Shultz, M. J. *J. Phys. Chem. B* **1997**, *101*, 10435−10441.
(20) Miyamae, T.; Morita, A.; Ouchi, Y. *Phys. Chem. Chem. Phys.* **2008**, *10*, 2010−2013.
(21) Ishiyama, T.; Morita, A. *J. Phys. Chem. C* **2011**, *115*, 13704−13716.
(22) Ishiyama, T.; Morita, A.; Miyamae, T. *Phys. Chem. Chem. Phys.* **2011**, *13*, 20965−20973.
(23) Petersen, P. B.; Saykally, R. J. *J. Phys. Chem. B* **2005**, *109*, 7976−7980.
(24) Mucha, M.; Frigato, T.; Levering, L. M.; Allen, H. C.; Tobias, D. J.; Dang, L. X.; Jungwirth, P. *J. Phys. Chem. B* **2005**, *109*, 7617−7623.
(25) Tarbuck, T. L.; Ota, S. T.; Richmond, G. L. *J. Am. Chem. Soc.* **2006**, *128*, 14519−14527.
(26) Levering, L. M.; Sierra-Hernandez, M. R.; Allen, H. C. *J. Phys. Chem. C* **2007**, *111*, 8814−8826.
(27) Tian, C. S.; Ji, N.; Waychunas, G. A.; Shen, Y. R. *J. Am. Chem. Soc.* **2008**, *130*, 13033−13039.
(28) Baldelli, S.; Schnitzer, C.; Campbell, D. J.; Shultz, M. J. *J. Phys. Chem. B* **1999**, *103*, 2789−2795.
(29) Jungwirth, P.; Curtis, J. E.; Tobias, D. J. *Chem. Phys. Lett.* **2003**, *367*, 704−710.
(30) Gopalakrishnan, S.; Jungwirth, P.; Tobias, D. J.; Allen, H. C. *J. Phys. Chem. B* **2005**, *109*, 8861−8872.
(31) Tarbuck, T. L.; Richmond, G. L. *J. Am. Chem. Soc.* **2006**, *128*, 3256−3267.
(32) Tian, C. S.; Byrnes, S. J.; Han, H. L.; Shen, Y. R. *J. Phys. Chem. Lett.* **2011**, *2*, 1946−1949.
(33) Hua, W.; Jubb, A. M.; Allen, H. C. *J. Phys. Chem. Lett.* **2011**, *2*, 2515−2520.
(34) Pegado, L.; Marsalek, O.; Jungwirth, P.; Wernersson, E. *Phys. Chem. Chem. Phys.* **2012**, *14*, 10248−10257.
(35) Tse, Y.-L. S.; Chen, C.; Lindberg, G. E.; Kumar, R.; Voth, G. A. *J. Am. Chem. Soc.* **2015**, *137*, 12610−12616.
(36) Perrin, D. D. *Ionization Constants of Inorganic Acids and Bases in Aqueous Solution*, 2nd ed.; Pergamon Press: New York, 1983.
(37) Yacovitch, T. I.; Wende, T.; Jiang, L.; Heine, N.; Meijer, G.; Neumark, D. M.; Asmis, K. R. *J. Phys. Chem. Lett.* **2011**, *2*, 2135−2140.
(38) Schnitzer, C. S.; Baldelli, S.; Shultz, M. J. *J. Phys. Chem. B* **2000**, *104*, 585−590.
(39) Jubb, A. M.; Allen, H. C. *J. Phys. Chem. C* **2012**, *116*, 13161−13168.
(40) Hua, W.; Verreault, D.; Adams, E. M.; Huang, Z. S.; Allen, H. C. *J. Phys. Chem. C* **2013**, *117*, 19577−19585.
(41) Huang, Z. S.; Hua, W.; Verreault, D.; Allen, H. C. *J. Phys. Chem. A* **2013**, *117*, 13412−13418.
(42) Ma, G.; Allen, H. C. *J. Phys. Chem. B* **2003**, *107*, 6343−6349.
(43) Tang, C. Y.; Allen, H. C. *J. Phys. Chem. A* **2009**, *113*, 7383−7393.
(44) Ji, N.; Ostroverkhov, V.; Tian, C. S.; Shen, Y. R. *Phys. Rev. Lett.* **2008**, *100*, 096102/1−096102/4.
(45) Nihonyanagi, S.; Yamaguchi, S.; Tahara, T. *J. Chem. Phys.* **2009**, *130*, 204704/1−204704/5.
(46) Chen, X. K.; Hua, W.; Huang, Z. S.; Allen, H. C. *J. Am. Chem. Soc.* **2010**, *132*, 11336−11342.
(47) Hua, W.; Verreault, D.; Allen, H. C. *J. Phys. Chem. Lett.* **2013**, *4*, 4231−4236.
(48) Hua, W.; Verreault, D.; Allen, H. C. *J. Phys. Chem. C* **2014**, *118*, 24941−24949.
(49) Hua, W.; Verreault, D.; Huang, Z.; Adams, E. M.; Allen, H. C. *J. Phys. Chem. B* **2014**, *118*, 8433−8440.
(50) Morita, A.; Hynes, J. T. *Chem. Phys.* **2000**, *258*, 371−390.
(51) Du, Q.; Superfine, R.; Freysz, E.; Shen, Y. R. *Phys. Rev. Lett.* **1993**, *70*, 2313−2316.
(52) Gopalakrishnan, S.; Liu, D. F.; Allen, H. C.; Kuo, M.; Shultz, M. J. *Chem. Rev.* **2006**, *106*, 1155−1175.
(53) Richmond, G. L. *Chem. Rev.* **2002**, *102*, 2693−2724.
(54) Tian, C. S.; Shen, Y. R. *Chem. Phys. Lett.* **2009**, *470*, 1−6.
(55) Sovago, M.; Campen, R. K.; Bakker, H. J.; Bonn, M. *Chem. Phys. Lett.* **2009**, *470*, 7−12.
(56) Ishiyama, T.; Morita, A. *J. Chem. Phys.* **2009**, *131*, 244714/1−244714/7.
(57) Pieniazek, P. A.; Tainter, C. J.; Skinner, J. L. *J. Am. Chem. Soc.* **2011**, *133*, 10360−10363.
(58) Xu, M.; Spinney, R.; Allen, H. C. *J. Phys. Chem. B* **2009**, *113*, 4102−4110.
(59) Nihonyanagi, S.; Kusaka, R.; Inoue, K.; Adhikari, A.; Yamaguchi, S.; Tahara, T. *J. Chem. Phys.* **2015**, *143*, 124707/1−124707/4.
(60) Casillas-Ituarte, N. N.; Callahan, K. M.; Tang, C. Y.; Chen, X. K.; Roeselova, M.; Tobias, D. J.; Allen, H. C. *Proc. Natl. Acad. Sci. U. S. A.* **2010**, *107*, 6616−6621.
(61) Tobias, D. J.; Stern, A. C.; Baer, M. D.; Levin, Y.; Mundy, C. J. *Annu. Rev. Phys. Chem.* **2013**, *64*, 339−359.
(62) Abramzon, A. A.; Gaukhberg, R. D. *Russ. J. Appl. Chem.* **1993**, *66*, 1473−1480.
(63) Abramzon, A. A.; Gaukhberg, R. D. *Russ. J. Appl. Chem.* **1993**, *66*, 1139−1146.
(64) Jungwirth, P.; Tobias, D. J. *J. Phys. Chem. B* **2001**, *105*, 10468−10472.
(65) Jungwirth, P.; Tobias, D. J. *Chem. Rev.* **2006**, *106*, 1259−1281.
(66) D'Auria, R.; Tobias, D. J. *J. Phys. Chem. A* **2009**, *113*, 7286−7293.
(67) Liu, D.; Ma, G.; Levering, L. M.; Allen, H. C. *J. Phys. Chem. B* **2004**, *108*, 2252−2260.
(68) Shen, Y. R. *The Principles of Nonlinear Optics*, 1st ed.; John Wiley & Sons: New York, 1984; p 563.


DOI: 10.1021/jacs.5b08636
*J. Am. Chem. Soc.* 2015, 137, 13920−13926